Sensors & Transducers, Vol. 273, Issue 2, June 2026, pp. 62-69

Sensors & Transducers

Published by IFSA Publishing, S. L., 2026
http://www.sensorsportal.com

Development of a Robotic Tool-Handling System for Decontamination in Nuclear Facilities

S. KAZEMI and S. GENTES

Karlsruhe Institute for Technology, Institute of Technology and Management in Construction,
Building 50.33, Am Fasanengarten, 76131 Karlsruhe, Germany
Tel.: +49 721 608-48235
E-mail: siavash.kazemi@kit.edu

Received: 1 April 2026 /Revised: 29 May 2026 /Accepted: 10 June 2026 /Published: 29 June 2026

Abstract: As part of the ROBDEKON [1] project, KIT-TMB is developing a robotic system for positioning two tools used in the decontamination and clearance measurement of concrete walls in nuclear power plants. To achieve this, a lifting platform (Manitou 100-VJR) was equipped with the necessary electronics-including controllers, sensors, actuators, communication modules, and safety systems-and converted into the robotic system "DecontBot" [2]. The machine can be operated in both teleoperation and (semi-)autonomous modes. Additionally, a graphical user interface (GUI) was designed for the DecontBot, allowing users to visualize the system in RViz2 on ROS2 and operate it in an intuitive, user-friendly manner. The DecontBot has been tested and evaluated by various personnel working in nuclear environments to gather feedback. This article provides a detailed description of the development steps of the DecontBot.

Keywords: Robotics, Automation, Decontamination, PLC, Robot operating system (ROS), Nuclear power plant (NPP).

1. Introduction

On April 15, 2023, the last three nuclear power plants in Germany-Emsland, Neckarwestheim 2, and Isar 2-were taken offline. Currently, there are 25 nuclear power plants and research reactors in the country at various stages of decommissioning and dismantling. Globally, it is estimated that around 297 nuclear power plants will begin the decommissioning process by 2030 [3].

To date, decommissioning and dismantling activities have been largely carried out manually. According to organizations such as the OECD, the current technological capabilities in dismantling are not being fully leveraged. By increasing the use of robots and automation technologies, it is possible not only to reduce costs but also to minimize radiation exposure for personnel involved in the process. Considering the large number of nuclear facilities undergoing dismantling, there is significant potential for digital and automated solutions in this field [4].

The ROBDEKON project, commissioned by the Federal Ministry of Research, Technology, and Space (BMFTR), aims to develop autonomous and semi-autonomous robotic solutions to improve safety and efficiency during decontamination in hazardous environments, including nuclear facilities. In collaboration with Karlsruhe University of Applied Sciences and the company Götting KG, KIT-TMB is developing an integrated chain for automating the decommissioning of nuclear power plants [5]. This chain consists of five steps and three robotic systems (see Fig. 1):

1. GammaBot – for environmental exploration, capturing geometric and radiological data;
2. Digitization – utilizing Building Information Modeling (BIM) for facility mapping;

3. Autonomous Decontamination and Clearance Measurement – performed with two robot-portable tools;
4. DecontBot – an autonomous carrier [6, 7];
5. Autonomous Waste Transportation handled by an autonomous forklift [8].

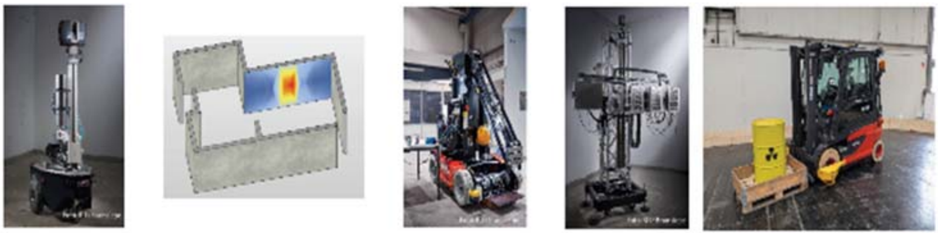

Fig. 1. Closed automated chain for decommissioning of NPPs.

The structure of this article is as follows: Section 2 details the development of the DecontBot, including both the adaptation of the original platform and the implementation of software and hardware components. Section 3 addresses the design of the human-machine interface, system visualization, and data communication while Section 4 describes the primary implementation of the control algorithm to automate the manipulator and Section 5 describes the automation of the vehicle. Section 6 presents the results of functional testing and summarizes feedback obtained from users. Finally, Section 7 provides the conclusions and an outlook on future developments.

A shorter version of this work appeared in ARCI 2026 [7]. This article extends it by introducing a vehicle-motion control framework, presenting initial experiments, and integrating manipulator and vehicle automation into a unified system-level study.

2. Development of DecontBot

To achieve the described objectives, the “Manitou 100-VJR” was further developed and automated as the base vehicle. The platform has approximate dimensions of 1.2 m in length, 1 m in width, and 2 m in height. Its manipulator, featuring three degrees of freedom (DOF), can reach up to 8 m in height with the aid of a telescopic joint and arm, and is capable of positioning tools weighing up to 270 kg.

2.1. Description of the Robot's Main Task

If the locations of hotspots or contaminations are identified using GammaBot, these areas must be decontaminated. To address this, KIT-TMB has developed an automated, robot-portable milling tool for decontaminating concrete walls [9]. Following decontamination, the surfaces are autonomously measured to verify that the contamination has been removed. For this purpose, a second tool, the “Contamination Array” [10], was developed. The primary function of the DecontBot is to position these two tools in either teleoperated or (semi-)autonomous modes [11].

The milling tool shown in Fig. 2 has two degrees of freedom, with a 2.2 kW motor driving the milling head for cutting and a 0.4 kW motor controlling its lateral motion. Safety features include digital switches and sensors that detect surface contact and the end of the milling trajectory, while a current sensor adjusts lateral speed to optimize cutting performance. The tool is powered by a 48 V battery, controlled via a Siemens CPU, and communicates with the DecontBot through UDP and TCP protocols, with a suction unit for dust and debris collection.

Fig. 2. Milling Tool.

The contamination array illustrated in Fig. 3 consists of four parallel detectors that are positioned precisely using linear drives, guided by a laser scanner to avoid obstacles and prevent self-contamination. Measurements are recorded digitally, including position, time, and radiological data, and can be monitored and managed.

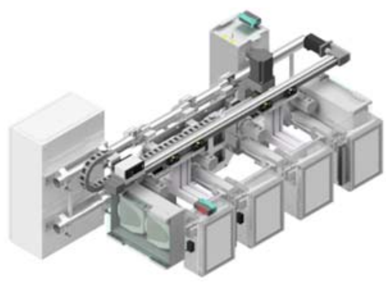

Fig. 3. Contamination Array.

Together, these tools enable the DecontBot to perform automated and safe decontamination and radiological assessment tasks in nuclear environments.

2.2. Description of the Integrated Electronics

The foundation of the automated decontamination system is the mobile platform described in Section 2.1. To transform this platform into a (semi-)automated decontamination system, it is first equipped with the necessary components. The control unit (PLC) is connected via a gateway to the sensors used to determine the positions of the manipulator and motor controllers.

The motor controllers, in turn, provide the PLC with essential feedback, including motor current, voltage, and temperature.

For positioning the decontamination system within its environment, two safety-rated LiDAR sensors are mounted on the platform. These sensors can also detect people or objects in the vicinity and, if necessary, trigger a warning signal or an emergency stop to prevent accidents or collisions.

In addition, the platform is equipped with other safety sensors, such as tilt sensors and safety switches, which generate warning signals when a hazard is detected. All warning signals are processed by a safety CPU on the PLC.

The safety system can be partially or fully overridden manually via the GUI if necessary; in such cases, the user receives a warning and assumes full responsibility for system operation.

Additional watchdog mechanisms are implemented to ensure safe communication among hardware components, including the PLC, control PC, operator PC, WLAN, and other connected devices.

Table 1 summarizes the key features and performance metrics of the integrated electronics.

Table 1. Performance metrics.

Cycle Time (PLC)	1 ms
Watchdog Response Time	2 ms
Safety Stop Distance	40 cm
Safety Warning Distance	60 cm
Manipulator Position Measurement Accuracy	Arm: 0.01° Turret: 0.05° Telescope: 0.1 mm
LiDAR Localization Accuracy	x: 0.01 mm y: 0.01 mm yaw: 0.1 °

3. GUI, HMI, Visualization and Data Transfer

The decontamination system is designed to operate in both teleoperation and autonomous modes, providing flexibility depending on the task requirements and the skill level of the operator. To ensure that the system can be used effectively without requiring extensive technical expertise, a user-friendly graphical interface has been developed. This interface allows operators to interact with the system intuitively, monitor its status in real-time, and make adjustments as needed.

In autonomous mode, the decontamination process is guided by the contamination map generated by GammaBot. Using this information, the DecontBot can automatically identify areas of contamination and accurately position its tools for decontamination or clearance measurement. The map data is transmitted directly from GammaBot to the DecontBot via a TCP server/client architecture, enabling seamless integration and continuous data exchange between the two systems.

Through the user interface (Fig. 4), operators can select, load, or delete available maps, initiate or stop the DecontBot, and switch between teleoperation and autonomous operation. The interface also provides critical real-time feedback, including safety release signals, collision warnings, and key system parameters such as manipulator joint positions, battery voltage, and localization status. The selected map is visualized in RViz2 on ROS2, allowing users to view both the 2D layout and the 3D point cloud of the building, alongside a dynamic URDF model of the DecontBot (Fig. 5).

Fig. 4. Graphical user interface (GUI).

This combination of autonomous guidance, real-time visualization, and intuitive control ensures that the DecontBot can operate efficiently and safely, even in complex and partially constrained nuclear environments. By providing operators with clear visualizations and system feedback, the interface reduces cognitive load, improves situational awareness, and allows for precise control of decontamination and measurement tasks. Furthermore, the integration of teleoperation and autonomous modes ensures that the system can adapt to a wide range of operational scenarios, from routine measurements to more challenging environments where human oversight is required.

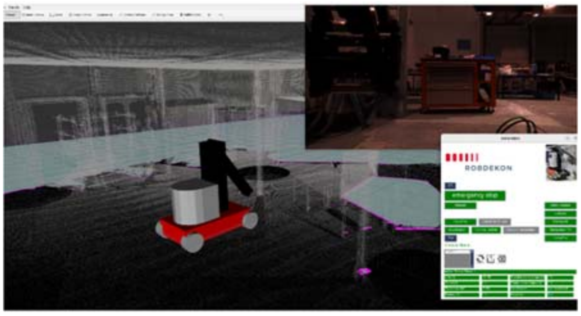

Fig. 5. Visualization via point cloud, camera image and URDF Model.

4. Automation of the Manipulator

For tasks such as robotic-assisted decontamination, ensuring that personnel remain outside hazardous working areas-or at a safe distance-is of paramount importance, often taking precedence over the degree of automation. This safety requirement can be addressed even in systems that rely primarily on teleoperation. Nevertheless, automation is highly recommended and frequently requested by users in the form of an assistant system to improve efficiency, precision, and overall workflow. Typical functionalities of such automation include autonomous navigation between rooms, execution of automated manipulation tasks, automatic positioning of the end effector at specified locations, returning the manipulator to a predefined home position, and independent automatic control of individual manipulator joints.

As illustrated in Fig. 4, the desired position of each manipulator joint can be specified directly through a graphical user interface, after which the manipulator moves to the corresponding configuration. Alternatively, a target point can be defined in task space using Cartesian coordinates, allowing the end effector to be commanded to the desired location. In this case, the desired task-space position is automatically transformed into joint-space positions for each joint through the manipulator's inverse kinematics. The details of the inverse kinematics equations are not included in this article, as they are standard and do not add significant insight to the presented methodology.

This dual approach-allowing both joint-space and task-space command-provides users with flexibility and precision when operating the manipulator, whether in teleoperation mode or during semi-autonomous and fully autonomous tasks. By combining intuitive interface controls with underlying kinematic transformations, the system ensures that manipulator movements are accurate, safe, and repeatable, reducing the risk of operator error while increasing the effectiveness of decontamination operations.

4.1. Controller Design for Manipulator

PID controllers are the most widely used controllers in industry, primarily due to their reliability and simplicity of implementation. In hydraulic systems-such as the manipulator of the DecontBot-where joint speeds are relatively low, the load acting on the end effector is nearly constant, and measurement noise is negligible or adequately filtered, the use of modern or adaptive control strategies is generally unnecessary. In most cases, classical controllers provide satisfactory performance after a one-time parameter tuning.

However, depending on the tool mounted on the DecontBot manipulator-such as a milling tool, contamination array, user-defined tool, or no tool at all-the load, which is directly related to the tool mass, can vary significantly. Consequently, different PID parameter sets are required for different operating conditions. To overcome this limitation, a two-degree-of-freedom (2-DOF) control structure is designed for each joint, consisting of a PI controller combined with a simple neural network-based controller [12], as illustrated in Fig. 6.

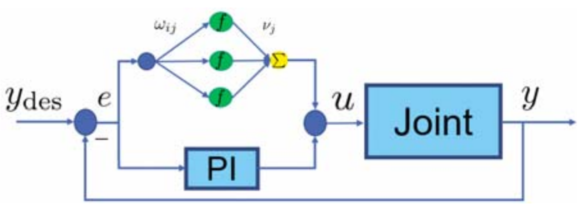

Fig. 6. 2-DOF control architecture with PI and neural network.

The PI component is primarily responsible for position control, while the neural network component provides corrective action by compensating for load-dependent variations in the system dynamics.

The input to the neural network component is the error dynamics, denoted by $I = [e]$.

The output of the hidden layer can be expressed as:

$$net_j^1 = f(I.\omega_{ij}), \quad (1)$$

and the output of the network can be expressed as:

$$u_{nn} = \sum_{j=1}^{M} \vartheta_j \,.\, net_j^1, \quad (2)$$

where i is an index of the network inputs, $e = y_{des} - y$ is a difference between desired position and actual position, $f(\cdot) = \tanh(\cdot)$ is an activation function, M is a number of neurons in the hidden layer, ω_{ij}, ϑ_j are network weights.

The total control law can be calculated as:

$$u = u_{nn} + u_{pi}, \quad (3)$$

or

$$\sum_{j=1}^{M} \vartheta_j \, . net_j^1 + k_p * e + k_i * \int e \, dt \quad (4)$$

The network parameters can be calculated and optimized online using backpropagation and gradient descent methods, as described in [12]. Table 2 shows the selected PI parameters of controller (4) for each joint and the corresponding position accuracies achieved.

Table 2. PI Parameters and results.

joint	Arm	Telescope	Turret
k_i	5	100	5
k_p.	8	500	12
accuracy	0.1 [°]	5 [mm]	2 [°]

It can be seen that the achieved accuracy of the turret is not fully satisfactory, which is due to the inherent positioning limitations of hydraulic systems caused by mechanical structure. Although this level of accuracy is sufficient for the current application, further improvements are planned to achieve an accuracy of less than 1°.

5. Automation of the Vehicle

Since the primary objective is to autonomously reach designated target points-specifically the contamination points-the vehicle must operate with a high degree of automation. The coordinates for these points are derived from a 3D contamination map generated by GammaBot, where the desired target points are defined as:

$$P_d = [x_d, y_d, z_d]^T \quad (5)$$

The operational workflow requires the vehicle to first navigate to an optimal 2D pose (x, y, θ) within the environment. Once the vehicle is positioned, the manipulator deploys the tools to the precise 3D target coordinates. It is important to note that the vehicle's mobile base may not always achieve the exact 2D coordinates required due to environmental constraints or positioning tolerances. In such cases, the manipulator must compensate by correcting the position not only along the z-axis but also within the x-y plane, provided the target remains within the robotic arm's reachable workspace.

A Point-to-Point (PTP) trajectory planning approach is utilized, which samples the optimal path through discrete iterations. This is implemented on the machine under the following convergence condition:

$$\|e(k)\| < \alpha, \quad (6)$$

where α is a small positive constant. Under this condition, the trajectory tracking problem is treated as a fixed-point control problem. The system advances to the next waypoint in the sequence only when the current tracking error is sufficiently small.

The following sections describe the automation logic and the implementation of the vehicle controller designed to transition the platform from one discrete waypoint to the next.

5.1. Controller Objectives for Vehicle

First step is to calculate distance and angle from start point and desired point as shown in Fig. 7.

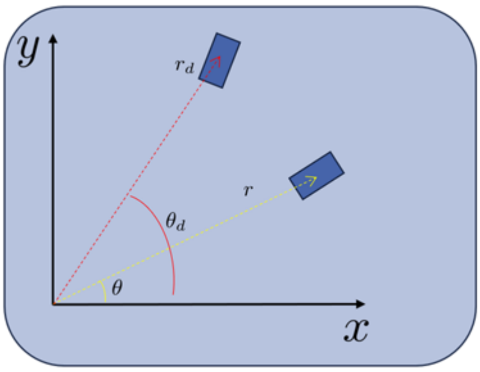

Fig. 7. Current vs. Desired Vehicle Position.

It can be seen that the vehicle needs to rotate from θ to θ_d and move along a distance equal to the magnitude of the vector $|r_d| - |r|$.

Therefore, the following error dynamics are to be minimized by the controller:

$$e_{rot} = \theta_d - \theta, \quad (7)$$

$$e_{lin} = |r_d| - |r|, \quad (8)$$

where θ and r are the current states of the Vehicle.

5.2. Motion Control Strategy

Fig. 8 illustrates the controller designed for the vehicle to perform linear motion. The control strategy uses a two-stage PI controller to ensure accurate and responsive motion.

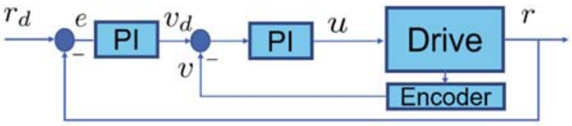

Fig. 8. Linear Motion Control.

First, the linear position error dynamics (difference between desired and current position) are fed into the first PI controller. The output of this controller is the desired velocity v_d for the vehicle. Using encoders, the current velocity v is continuously measured and compared to the desired velocity. The difference between these two signals, defined as the velocity error dynamics, is then used as the input to a second PI controller, which generates the control signal u. This signal u is ultimately implemented as the PWM applied to the drive motors.

This two-stage control strategy is necessary because using a single PI controller (where $u = f(e_{\text{lin}})$) can lead to very slow motion near the end of a trajectory, especially when Δr or e_{lin} is small, since the PWM would become too low to drive the motors effectively. By introducing the intermediate velocity control, the desired velocity is maintained at a sufficient level, ensuring the PWM signal remains strong enough to overcome friction, inclines, or obstacles, even when the position error is small. This allows the vehicle to maintain responsiveness and stability throughout the motion.

Unlike linear motion, the orientation control of the vehicle around the $\boldsymbol{z}$-axis is implemented using a single PD controller.

$$u = k_p * e_{rot} + k_d * \dot{e}_{rot} \tag{9}$$

The derivative (D) component in the PD controller is essential for controlling the vehicle's orientation around the $\boldsymbol{z}$-axis. Without this component, the vehicle exhibits significant overshoot, and the orientation response tends to resemble a sinusoidal oscillation around the desired angle $\boldsymbol{\theta_d}$. Such oscillatory behavior is caused by the system's inertia and the lack of damping in the control loop, which allows the vehicle to continuously overshoot the target orientation before eventually settling. By incorporating a properly tuned D term, these oscillations are effectively damped, providing additional resistance to rapid changes in angular velocity. As a result, the vehicle achieves smooth and stable convergence to the target orientation, with minimal overshoot and reduced settling time.

The choice and tuning of controller parameters are critical in achieving this performance. Table 3 summarizes the parameters of the controllers used for both linear motion and rotational control of the vehicle. These parameters were carefully selected to balance responsiveness and stability: the proportional components ensure the vehicle reacts appropriately to position and orientation errors, while the integral component in the linear motion controller eliminates steady-state errors, and the derivative component in the rotational controller mitigates oscillatory behavior. Together, these settings allow the vehicle to follow the desired trajectory accurately while maintaining smooth and stable motion in both translation and rotation.

Table 3. Parameters of the Controllers.

joint	Linear	Rotational
k_p	900	45
k_d	-	12
k_i	25	-

5.2. Tests and First Control Results

As an initial test, the vehicle was required to move from the starting position [2.712 m, 0.414 m] with an orientation of $\theta = 4.08°$ to the target position [6 m, 1 m] with a desired orientation of $\theta_d = 6°$. Fig. 9 illustrates the start and end positions of the vehicle after completing the movement. After executing the trajectory, the vehicle reached a final position of [5.976 m, 0.9828 m] with $\theta = 4.46°$. These results indicate that the vehicle performs well in terms of linear positioning, achieving a final position very close to the desired target.

While the orientation is slightly off from the desired value, the overall performance of the vehicle in following the planned path is satisfactory for an initial test, demonstrating the effectiveness of the implemented control strategy for basic linear motion.

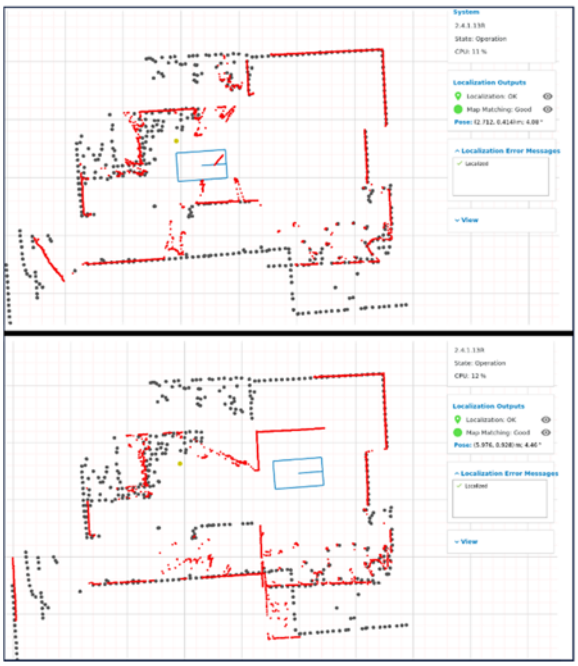

Fig. 9. Start position (top) versus end position (bottom) of the vehicle.

Achieving exact orientation for mobile vehicles with hydraulic steering is inherently challenging, especially when the required change in orientation is small, due to the limited steering dynamics. Therefore, further work on the vehicle's rotational control is needed to reduce the orientation error dynamics below an acceptable threshold.

In cases of larger orientation changes, for example $\Delta\theta = 20°$, the steady-state error remains around 1-2°. A more extensive analysis or statistical evaluation of the remaining error is not provided in this work, as the controller design is still in progress and will be addressed in future studies.

6. Primary Test Results

Understanding the opinions and experiences of actual users is crucial for improving the functionality and acceptance of any engineering system, and the DecontBot is no exception. To gather such feedback, the DecontBot-equipped with its secondary tool, the Contamination Array-was tested in a controlled nuclear laboratory environment at the Institute of Nuclear Waste Disposal (KIT-INE). The primary aim of these tests was to evaluate the system's usability, effectiveness, and overall user experience under realistic operational conditions.

A total of five testers, all professionals working in the field of nuclear engineering but without specialized robotics experience, participated in the evaluation. Each tester interacted with the system for approximately 30 minutes. During this period, the users positioned the contamination array to specific locations and initiated clearance measurements via teleoperation. It is important to note that only the positioning of the tool was controlled manually via teleoperation, while the measurement process itself was carried out automatically by the tool. This separation ensured that the evaluation focused on the human-machine interaction aspects rather than the automated measurement capabilities.

Due to data protection and safety requirements, further details regarding the layout and general characteristics of the testing environment cannot be disclosed in this work. Nonetheless, the testing setup provided sufficient realism to assess the system's practical usability.

In addition to the hands-on evaluation, the users completed a questionnaire consisting of 15 questions, designed to capture detailed feedback on multiple aspects of the system. The questionnaire addressed five categories: general impression, usability, work support, safety and trust, and fun factor. It also included open-ended sections where users could provide suggestions for improvement, such as the implementation of an adjustable step speed for teleoperation. All responses were recorded on a Likert scale from 1 to 5, and the aggregated results are summarized in Fig. 10, providing a visual overview of user ratings across all categories.

Additional tests with other users were also conducted, although these are not described in detail here. Overall, the results were highly encouraging, with the system exceeding expectations in most categories. The fun factor received the highest rating, highlighting the engaging and interactive nature of the system; however, it was observed that this rating tends to decrease slightly as users become more familiar with the system and the tasks begin to feel repetitive. Conversely, increased practice and familiarity led to noticeable improvements in usability and overall impression, suggesting that the system becomes more intuitive and efficient with repeated use. These findings underscore the importance of iterative testing and user feedback in optimizing both the functionality and user experience of complex robotic systems like the DecontBot.

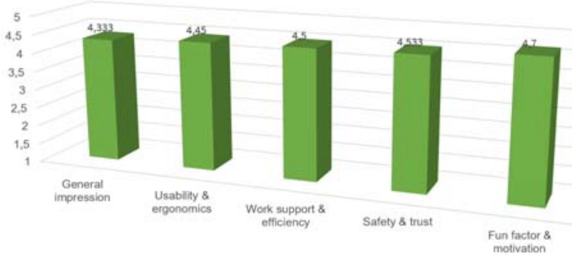

Fig. 10. Test results and user ratings.

7. Conclusions and Further Developments

The mechanical and electrical upgrades of the DecontBot have already been completed, and the platform can currently be operated in teleoperation mode. The next step involves the integration of path planning and advanced control algorithms to enable fully autonomous operation of the vehicle, as the manipulator control has already been successfully implemented. In particular, the control of the vehicle's driving and navigation needs further refinement to ensure precise and smooth movement, especially in complex environments with tight spaces, inclined surfaces, or obstacles. Improvements in driving control will enhance the platform's overall stability, responsiveness, and accuracy, allowing it to follow planned paths reliably without continuous manual intervention.

In addition to autonomous navigation, further degrees of freedom will be added to the end effector to allow more precise positioning of the decontamination and clearance measurement tools on inclined walls, floors, and ceilings. These enhancements will enable the DecontBot to reach areas that are difficult or unsafe for human operators, increasing both the versatility and effectiveness of the platform. The platform's safety will also be thoroughly evaluated and certified by TÜV (Technical Inspection Association), ensuring compliance with rigorous operational and occupational safety standards.

Future tests are planned to encompass not only measurement tasks but also actual decontamination operations using a milling tool. Automation and robot-based solutions have already demonstrated significant potential in decontamination work: they relieve personnel from physically demanding and hazardous tasks, while simultaneously helping to minimize the generation of secondary waste. The DecontBot was therefore specifically developed for the decontamination and clearance measurement of concrete walls in nuclear power plants. By employing the DecontBot, both the effort and the risk associated with these operations can be substantially reduced, making such work safer, faster, and more efficient.

There is strong interest among nuclear power plant operators in adopting autonomous or robotic systems for decontamination work, particularly as these solutions offer the dual benefit of reducing human exposure to radioactive materials and increasing the precision and reliability of decontamination processes. Further development of the driving and navigation control, combined with enhanced tool positioning and autonomous path planning, will be essential to fully realize the potential of the DecontBot and similar robotic platforms in industrial nuclear environments.

References

[1]. J. Petereit, et al., ROBDEKON: Robotic systems for decontamination in hazardous environments, in *Proceedings of the IEEE International Symposium on Safety, Security, and Rescue Robotics (SSRR)*, 2019, pp. 16-23.

[2]. S. Kazemi, S. Gentes, Development of a robot system as a tool-carrier machine for the decontamination process of nuclear power plants, in *Proceedings of the 5th Winter IFSA Conference on Automation, Robotics & Communications for Industry 4.0/5.0 (ARCI)*, 2025, pp. 47-52.

[3]. KernD, Kernkraftwerke außer Betrieb: Leistung und erzeugter Strom, https://www.kernd.de/kernd/themen/strom/Zahlen-und-Fakten/01_index.php#anchor_27a91b5f_Accordion-Kernkraftwerke-ausser-Betrieb (in German).

[4]. A. D. Little, Statista, Rückbau von Kernkraftwerken weltweit bis zum Jahr 2030, https://de.statista.com/statistik/daten/studie/201684/umfrage/rueckbau-von-kernkraftwerken-weltweit/ (in German).

[5]. S. Gentes, et al., From environmental exploration to clearance measurement – developing mobile robot systems for decommissioning of nuclear power plants, *at - Automatisierungstechnik*, Vol. 70, Issue 10, 2022, pp. 886-896.

[6]. S. Kazemi, Robotic automation for nuclear decommissioning: Development of a tool carrier system with milling and clearance measurement capabilities, *Sensors & Transducers*, Vol. 268, Issue 1, 2025, pp. 28-36.

[7]. S. Kazemi, S. Gentes, Design and development of a robotic tool-carrier for nuclear power plant decontamination, in *Proceedings of the 6th Winter IFSA Conference on Automation, Robotics & Communications for Industry 4.0/5.0/6.0 (ARCI)*, 2026, pp. 24-27.

[8]. Götting KG, Hannover Messe 2024, https://www.goetting.de/hannover-messe-2024/ (in German).

[9]. C. Li, S. Kazemi, S. Gentes, Development of an automated milling system for the decontamination of the wall surface in a nuclear power plant, *Safety of Nuclear Waste Disposal*, Vol. 1, 2021, pp. 23-24.

[10]. A. Wernke, Automatisierung der Kontaminationsmessung im Rückbauprozess kerntechnischer Anlagen, *atw – International Journal for Nuclear Power*, Vol. 67, Issue 5, 2022 (in German).

[11]. S. Kazemi, S. Gentes, Development of a robotic system for the automation of the decontamination process of nuclear power plants, *Safety of Nuclear Waste Disposal*, Vol. 2, 2023, pp. 13-14.

[12]. S. Kazemi, S. Gentes, Self-constructing neural network controllers with adaptive structural learning: Application to stepper motor positioning, in *Proceedings of the 13th International Conference on Control, Mechatronics and Automation (ICCMA)*, 2025, pp. 231-236.